Uniform Description of Soft Observables in Heavy-Ion Collisions at $\sqrt{s_{NN}} = 200$ GeV

Wojciech Broniowski,[1,2] Mikolaj Chojnacki,[1] Wojciech Florkowski,[1,2] and Adam Kisiel[3,4]

[1]The H. Niewodniczański Institute of Nuclear Physics, Polish Academy of Sciences, PL-31342 Kraków, Poland
[2]Institute of Physics, Jan Kochanowski University, PL-25406 Kielce, Poland
[3]Faculty of Physics, Warsaw University of Technology, PL-00661 Warsaw, Poland
[4]Department of Physics, Ohio State University, Columbus, Ohio 43210, USA

(Received 28 January 2008; revised manuscript received 30 April 2008; published 8 July 2008)

We investigate the hydrodynamic evolution of the system formed in ultrarelativistic heavy-ion collisions and find that an appropriate choice of the initial condition, specifically a simple two-dimensional Gaussian profile for the transverse energy, in conjunction with a realistic equation of state, leads to a uniform description of soft observables measured at the relativistic heavy-ion collider. In particular, the transverse-momentum spectra, the elliptic-flow, and the Hanbury-Brown–Twiss correlation radii, including the ratio $R_{\mathrm{out}}/R_{\mathrm{side}}$ as well as the dependence of the radii on the azimuthal angle, are all properly described.

DOI: 10.1103/PhysRevLett.101.022301 PACS numbers: 25.75.Ld, 25.75.Dw, 25.75.Gz

The notorious difficulties in simultaneous description of various features of the soft hadron production in the nucleus-nucleus collisions at RHIC are well known [1]. In particular, the so called RHIC puzzle [1–4] refers to problems in reconciling the large value of the elliptic-flow coefficient, v_2, with the Hanbury-Brown–Twiss (HBT) interferometry in numerous approaches including hydrodynamics [5–9]. In these approaches, which conventionally use the initial transverse profile from Glauber calculations, the description of v_2 favors longer hydrodynamic evolution times, while the HBT radii, sensitive to the size and life-time of the system, are reproduced when the evolution time is short. In particular, the ratio of the out to side radius obtained from hydrodynamics has been 25%–50% above the data, thus posing a major difficulty for the credibility of the hydrodynamic approach. In this Letter we show that this puzzle may be resolved with a proper choice of initial condition for hydrodynamics in conjunction with the realistic equation of state and the inclusion of all resonances in the modeling of freeze-out.

The basic finding of this work is that the choice of the initial condition for hydrodynamics is a very important element. Ideally, and this remains a challenge, the initial density and flow profiles should be provided by the early dynamics, for instance the color glass condensate [10,11]. In practice, however, the theory of the partonic stage carries some uncertainty in its parameters, moreover, there may exist other effects in the early dynamics, see, e.g., [12,13]. It is then practical to use a simple parameterization of the initial profile. Here we investigate boost-invariant systems, which approximate well the RHIC collisions at midrapidity. We take the Gaussian initial energy-density profile of the system in the transverse plane (x, y) at the initial proper time $\tau_0 = 0.25$ fm (we use $c = 1$ throughout this Letter),

$$n(x, y) = \exp\left(-\frac{x^2}{2a^2} - \frac{y^2}{2b^2}\right). \qquad (1)$$

The values of the a and b width parameters depend on the centrality class and are obtained by matching to the results for $\langle x^2\rangle$ and $\langle y^2\rangle$ from GLISSANDO [14], which implements the eccentricity fluctuations of the system in the Glauber approach [15,16]. Essentially, $(a^2 + b^2)/2$ describes the overall transverse size of the system, while $(b^2 - a^2)/(b^2 + a^2)$ parameterizes its eccentricity. The use of the Gaussian profile (1) results in a stronger transverse flow as compared to the Glauber initial conditions, which is crucial for the success of the approach. The values for centrality classes used in this work are collected in Table I. The energy-density profile (1) determines the temperature profile via the equation of state [17]. The initial central temperature, T_i, dependent on centrality, is adjusted to reproduce the total pion multiplicity.

The hydrodynamics used is inviscid, baryon-free, and boost invariant. The equation of state is taken to be as realistic, as possible. We use the lattice-QCD simulations of Ref. [18] at high temperatures, $T > 170$ MeV, the hadronic gas including explicitly all resonances from the particle data tables as implemented in SHARE [19] at $T < 170$ MeV, and a smooth interpolation in the vicinity of 170 MeV, which implements the smooth crossover. In fact, only the temperature dependence of the sound velocity c_s, shown Fig. 1, is relevant, as all other thermodynamic quantities follow from it [17] via thermodynamic identities. The equations are solved with the technique of Ref. [20]. The entropy-conservation test is satisfied at the relative level of 10^{-5} or better, proving the numerical accuracy of the method.

TABLE I. Shape parameters of Eq. (1) for various centrality classes used in this work.

c [%]	0–5	20–30	20–40
a [fm]	2.65	1.94	1.78
b [fm]	2.90	2.52	2.45

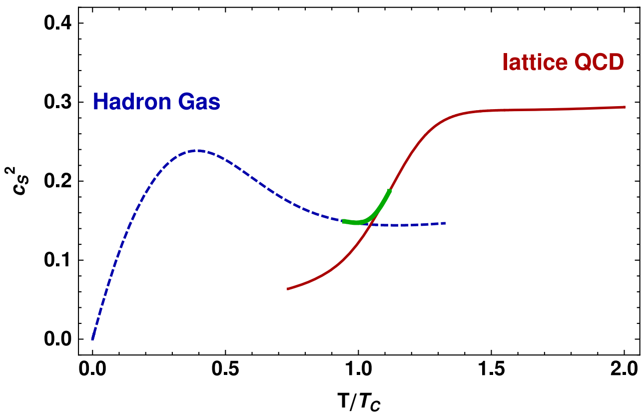

FIG. 1 (color online). Temperature dependence of the sound velocity squared. A smooth crossover is implemented between the high-temperature lattice-QCD region and the low-temperature hadronic gas region.

At the temperature $T_f = 145$ MeV (model parameter) the system freezes and hadrons (stable and resonances) are generated according to the standard Cooper-Frye formalism [21]. Lower values of T_f lead to larger sizes of the system and larger transverse flow. This in turn results in flatter p_T spectra and larger splitting of the v_2 of pions or kaons and protons. The freeze-out hypersurfaces for two centrality classes are shown in Fig. 2. We note a similarity of their volume-emission parts (with timelike normal vectors) to the blast-wave parameterization [22], with a short lifetime: about 9 fm for central ($c = 0$–5%) and 7 fm for midperipheral ($c = 20\%$–30%) collisions. However, our freeze-out hypersurfaces contain also the surface emission parts (with spacelike normal vectors), absent in the traditional blast-wave parameterizations. We have checked that the potential problems from the noncausal surface emission [23–25], are negligible, as less than 0.5% of particles are emitted back into the hydrodynamic region. The reason for this very small fraction is the sizable transverse flow velocity at large radii, as indicated by labels in Fig. 2, which pushes the particles outward, as well as the fact that the hypersurfaces are not bent back at low values of t. We have determined that about half of the produced particles comes from the volume part and about half from the surface part of the freeze-out hypersurface. The surface emission is crucial for fitting the HBT data from RHIC, as also advocated in [26,27].

For comparison, in Fig. 3 we show the hypersurfaces obtained in a calculation of [28] performed with the commonly used *Glauber* initial condition (and with the same equation of state). Following the same strategy as in this work, the parameters were adjusted in such a way that the soft observables are globally described as closely as possible. Similarly to other hydrodynamic studies, it was impossible to reach as good agreement as in this work, with the HBT radii described at the level of 15%–20% only. The ratio $R_{\mathrm{out}}/R_{\mathrm{side}} \sim 1.25$ in [28], while typically reaching the values around 1.5 in other hydrodynamic

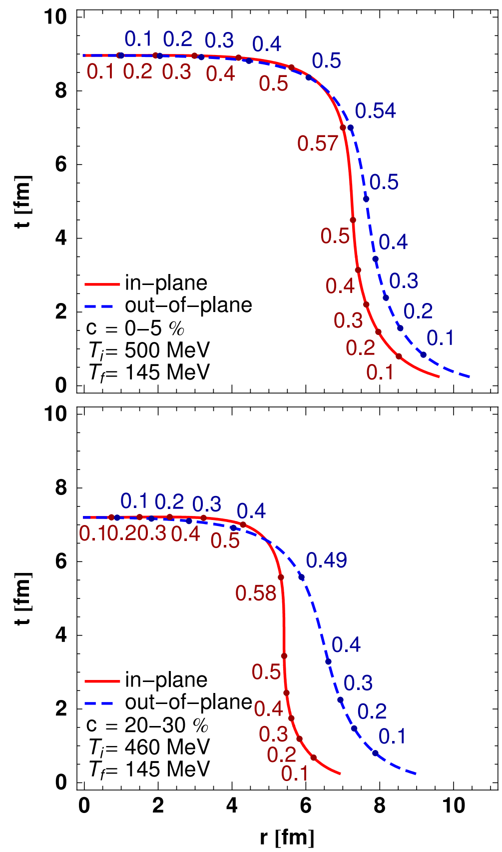

FIG. 2 (color online). Freeze-out hypersurfaces for $c = 0\%$–5% (top) and $c = 20\%$–30% (bottom), obtained with the condition $T_f = 145$ MeV. The two curves show the in-plane and out-of-plane sections. The labels indicate the transverse flow velocity.

calculations. The reason for this difference, or for the success of the present approach, can be seen by comparing Fig. 3 and bottom of Fig. 2. We note that the Glauber initial condition results in hypersurfaces of a smaller transverse

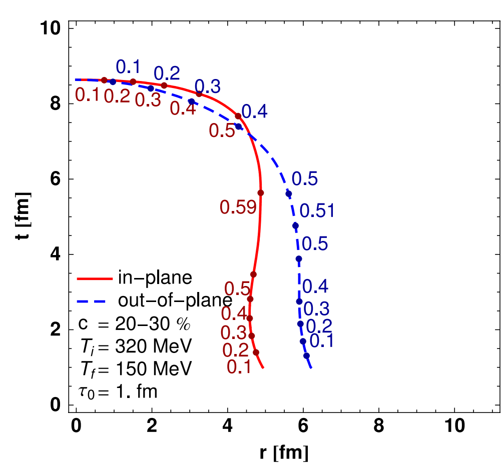

FIG. 3 (color online). Freeze-out hypersurfaces for $c = 20\%$–30% for the calculation starting from the Glauber initial condition with parameters optimized to fit the data as described in [28]. Notation as in Fig. 2.

size and a longer evolution time, which translates into lower R_{side} and larger R_{out}. More generally, we note a quite different shape of the hypersurfaces in Figs. 2 and 3, however, the flow values are similar, which results from the fact that the model parameters are adjusted in such a way that the slopes of the p_T-spectra and the v_2 coefficient are reproduced. This leads to practically the same values of the flow velocity at freeze-out for the two compared calculations.

Possible elastic rescattering processes among hadrons after freeze-out are neglected, thus they stream freely, with the resonances decaying on the way. This stage is simulated with THERMINATOR [29], which incorporates all resonances from the particle data tables. The collision rate after freeze-out is not very large for the obtained hypersurfaces. It can be estimated as follows: one considers a pion straight-line trajectory and counts the number of collisions, i.e., the encounters with other particles closer than the distance corresponding to the cross section. Averaging over all pions yields the number of these trajectory crossings about 1.5–1.7 per pion. Hence the single-freeze-out scenario [30] seems to be a fairly good approximation for the present case. The use of hadronic afterburners modeling the elastic collisions has been described, e.g., in [31–33].

Our results for central and midperipheral collisions with the centrality classes adjusted to the available PHENIX [34,35] and STAR [36] data are shown in Figs. 4 and 5. We note a uniform agreement for all soft phenomena studied. In particular, the transverse-momentum spectra, the pionic elliptic flow, and the HBT radii, including the ratio $R_{\text{out}}/R_{\text{side}}$, are properly described. The dependence of the HBT quantities on the transverse momentum of the pair, k_T, is correct. The value of R_{long} is slightly too large, which may be due to the boost-invariant approximation. We note that we use the two-particle method with the Coulomb corrections described in [37] for the femtoscopy. This approach follows closely the experimental procedures, thus is most appropriate when comparing to the data. The results obtained for other centralities are of similar quality as those in Figs. 4 and 5. We conclude that the choice of the initial profile (1) is crucial for this agreement, with the reasons mentioned in the discussion of Figs. 2 and 3 above.

Having properly described the HBT radii, we may deal "as a bonus" with the azimuthally sensitive HBT interferometry [38] and consider the second-order Fourier coef-

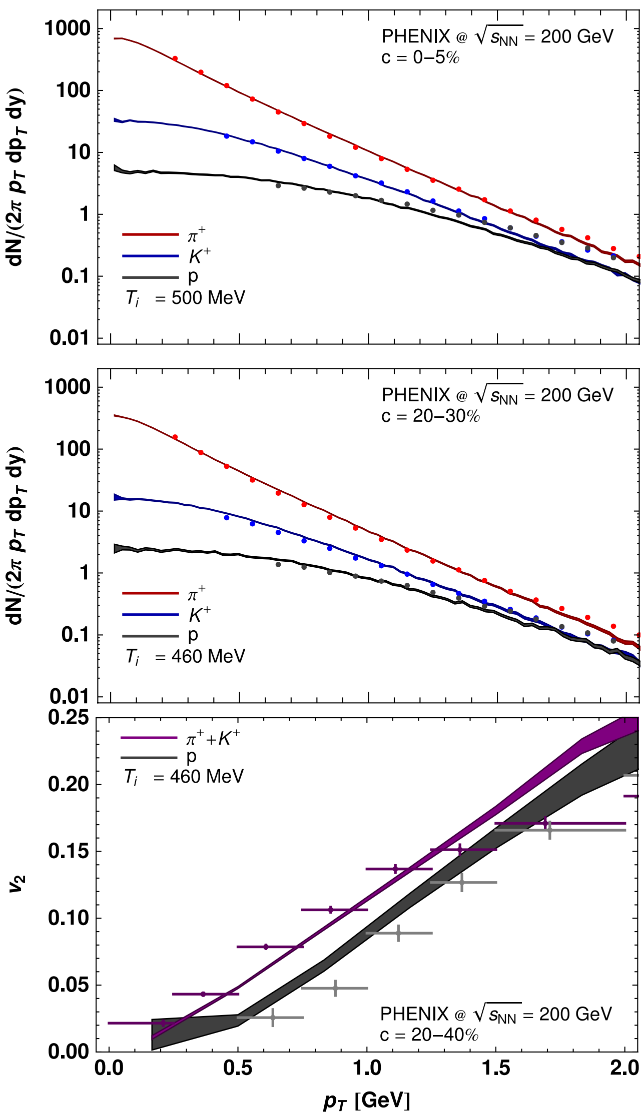

FIG. 4 (color online). The transverse-momentum spectra of pions, kaons and protons for $c = 0\%–5\%$ (upper panel), $c = 20\%–30\%$ (middle panel), and the elliptic-flow coefficient v_2 for $c = 20\%–40\%$ (lower panel), plotted as functions of the transverse momentum and compared to the data from [34,35].

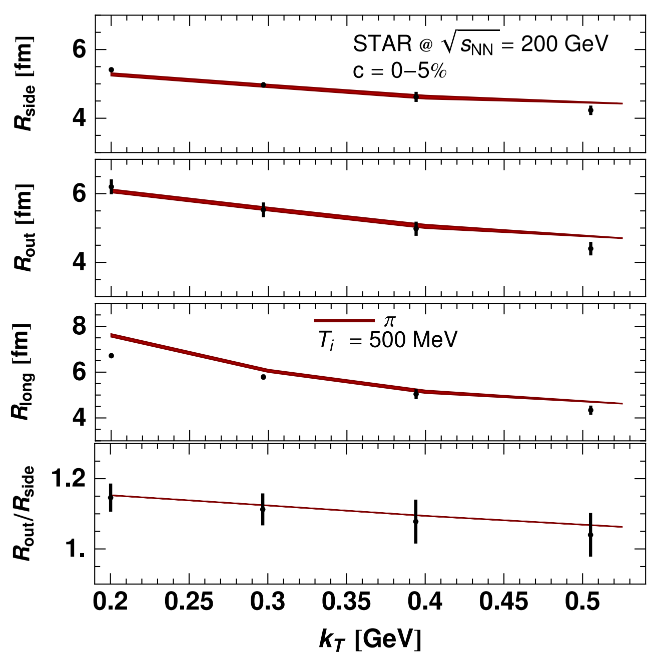

FIG. 5 (color online). The pion HBT radii R_{side}, R_{out}, R_{long}, and the ratio $R_{\text{out}}/R_{\text{side}}$ for central collisions, compared to the data from [36].

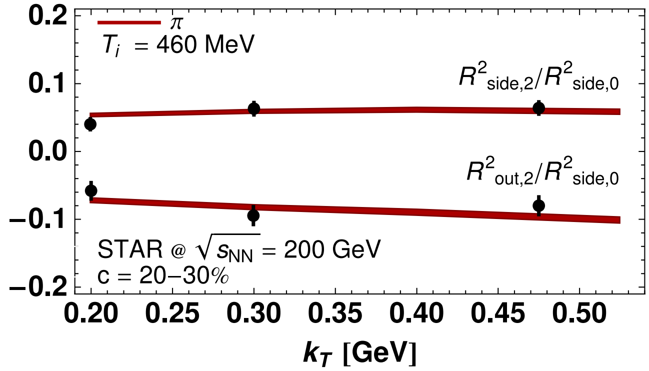

FIG. 6 (color online). $R^2_{\mathrm{side},2}/R^2_{\mathrm{side},0}$ and $R^2_{\mathrm{out},2}/R^2_{\mathrm{side},0}$ from the model (bands) and experiment [38] (points), plotted as functions of the transverse momentum of the pion pair.

ficients defined as the averages over the azimuthal angle, $R^2_{i,2}(k_T) = \langle R^2_i(k_T, \varphi)\cos(2\varphi)\rangle$, where $i =$ side or out ($R_{2,\mathrm{long}} = 0$). The results shown in Fig. 6 display a remarkable agreement between our model and the data.

In conclusion: (i) With a proper choice of the initial profile (Gaussian) and a realistic equation of state one may obtain a uniform description of the soft observables (p_T-spectra, v_2, and pionic HBT radii) at RHIC, solving the "RHIC HBT puzzle." Two elements are crucial here: the initial profile (1) and the equation of state with the crossover phase transition. The resulting hypersurfaces at freeze-out have relatively short evolution times and larger transverse sizes, which allows to properly reproduce the HBT data. (ii) Azimuthally-sensitive HBT is described in agreement with the data. (iii) The inclusion of all resonances in the hadronic phase is important, as has been well known from other calculations in statistical models. (iv) The backward emission problem for the obtained freeze-out hypersurfaces is negligible. (v) The obtained realistic picture of the space-time evolution of the fireball may be used for further studies, e.g., modeling of hard-probe dynamics such as jet quenching.

This work was supported by the Polish Ministry of Science and Higher Education, Grants N202 153 32/4247 and N202 034 32/0918, and by the U.S. NSF Grant No. PHY-0653432.

[1] U. W. Heinz and P. F. Kolb, arXiv:hep-ph/0204061.
[2] T. Hirano, Acta Phys. Pol. B **36**, 187 (2005).
[3] M. A. Lisa, S. Pratt, R. Soltz, and U. Wiedemann, Annu. Rev. Nucl. Part. Sci. **55**, 357 (2005).
[4] P. Huovinen and P. V. Ruuskanen, Annu. Rev. Nucl. Part. Sci. **56**, 163 (2006).
[5] U. W. Heinz and P. F. Kolb, Nucl. Phys. **A702**, 269 (2002).
[6] T. Hirano, K. Morita, S. Muroya, and C. Nonaka, Phys. Rev. C **65**, 061902 (2002).
[7] T. Hirano and K. Tsuda, Nucl. Phys. **A715**, 821 (2003).
[8] D. Zschiesche, S. Schramm, H. Stoecker, and W. Greiner, Phys. Rev. C **65**, 064902 (2002).
[9] O. Socolowski, Jr., F. Grassi, Y. Hama, and T. Kodama, Phys. Rev. Lett. **93**, 182301 (2004).
[10] L. D. McLerran and R. Venugopalan, Phys. Rev. D **49**, 2233 (1994); **49**, 3352 (1994).
[11] D. Kharzeev, E. Levin, and M. Nardi, Phys. Rev. C **71**, 054903 (2005).
[12] S. Mrówczyński, Phys. Lett. B **314**, 118 (1993).
[13] B. Muller, arXiv:0710.3366.
[14] W. Broniowski, M. Rybczyński, and P. Bożek, arXiv:0710.5731.
[15] R. Andrade *et al.*, Phys. Rev. Lett. **97**, 202302 (2006).
[16] Y. Hama *et al.*, arXiv:0711.4544.
[17] M. Chojnacki and W. Florkowski, Acta Phys. Pol. B **38**, 3249 (2007).
[18] Y. Aoki, Z. Fodor, S. D. Katz, and K. K. Szabo, J. High Energy Phys. 01 (2006) 089.
[19] G. Torrieri *et al.*, Comput. Phys. Commun. **167**, 229 (2005).
[20] M. Chojnacki and W. Florkowski, Phys. Rev. C **74**, 034905 (2006).
[21] F. Cooper and G. Frye, Phys. Rev. D **10**, 186 (1974).
[22] E. Schnedermann, J. Sollfrank, and U. W. Heinz, Phys. Rev. C **48**, 2462 (1993).
[23] K. A. Bugaev, Nucl. Phys. **A606**, 559 (1996).
[24] C. Anderlik *et al.*, Phys. Rev. C **59**, 3309 (1999).
[25] M. S. Borysova *et al.*, Phys. Rev. C **73**, 024903 (2006).
[26] Y. M. Sinyukov, Acta Phys. Pol. B **37**, 3343 (2006).
[27] M. Gyulassy, Y. M. Sinyukov, I. Karpenko, and A. V. Nazarenko, Braz. J. Phys. **37**, 1031 (2007).
[28] M. Chojnacki, W. Florkowski, W. Broniowski, and A. Kisiel, arXiv:0712.0947 [Phys. Rev. C (to be published)].
[29] A. Kisiel, T. Taluc, W. Broniowski, and W. Florkowski, Comput. Phys. Commun. **174**, 669 (2006).
[30] W. Broniowski and W. Florkowski, Phys. Rev. Lett. **87**, 272302 (2001).
[31] D. Teaney, J. Lauret, and E. V. Shuryak, Phys. Rev. Lett. **86**, 4783 (2001).
[32] C. Nonaka and S. A. Bass, Phys. Rev. C **75**, 014902 (2007).
[33] T. Hirano, U. W. Heinz, D. Kharzeev, R. Lacey, and Y. Nara, J. Phys. G **34**, S879 (2007).
[34] S. S. Adler *et al.* (PHENIX Collaboration), Phys. Rev. C **69**, 034909 (2004).
[35] S. S. Adler *et al.* (PHENIX Collaboration), Phys. Rev. Lett. **91**, 182301 (2003).
[36] J. Adams *et al.* (STAR Collaboration), Phys. Rev. C **71**, 044906 (2005).
[37] A. Kisiel, W. Florkowski, and W. Broniowski, Phys. Rev. C **73**, 064902 (2006).
[38] J. Adams *et al.* (STAR Collaboration), Phys. Rev. Lett. **93**, 012301 (2004).